Synthesis and Characterization of Nanosized Halogenated and Interhalogenated Metal Oxide Adducts

Johanna A. Haggstrom,[†] Peter K. Stoimenov,[‡] and Kenneth J. Klabunde*,[†]

Department of Chemistry, Kansas State University, Manhattan, Kansas 66506, and Department of Chemistry, University of California at Santa Barbara, Santa Barbara, California 93106

Received January 9, 2008. Revised Manuscript Received March 10, 2008

Nonpolar halogens (Cl_2, Br_2, and I_2) and polar interhalogen molecules (ICl, IBr, and ICl_3) have been adsorbed on the surface of three different nanosized metal oxides (NanoActive (NA) Al_2O_3 Plus, NA-TiO_2, and NA-CeO_2). The prepared halogen and interhalogen adducts have been characterized in detail by thermogravimetric analysis (TGA), UV−vis, Raman, and X-ray photoelectron spectroscopies (XPS), and the results are discussed herein. The different metal oxides lead to varying strength of adsorption of the halogen/interhalogen in the prepared adducts. Adsorption was also tested on their macrocrystalline available counterparts but with no success. Nanosized metal oxide halogen adducts possess high surface reactivities due to their unique surface morphologies. These adducts can be used as halogenating agents in organic and inorganic synthesis, for disinfection and decontamination.

Introduction

Nanomaterials have been carefully studied in the past several years, and new areas of use are frequently discovered. Their intriguing chemical properties arise from the presence of numerous corners, edges, and defect sites, which lead to unique surface morphologies and reactive surface ions or atoms. The characteristic morphology of nanosized materials becomes very important in solid-state interactions, where the morphology of the surface dictates the reactivity of the material. Nanosized metal oxides have been extensively studied,[1–7] mainly for their use as destructive adsorbents,[1,3,4,6] and for their role in catalysis.[2,7] One of the most recent interests has involved using nanoparticles for decontamination of vegetative bacterial cells and spores,[4,8–10] and to increase the biocidal activity of the nanosized metal oxide, halogen has been adsorbed on the surface,[8,11] which is also a safe and efficient method to store elementary halogen.[11]

Several published articles have described the interaction of halogen and interhalogen molecules on the surface of MgO, using quantum calculations and molecular dynamics simulations.[12–17] It was found that the photodissociation of I_2,[15,16] ICl,[14,16] and IBr[17] can be significantly changed by adsorption on a magnesium oxide surface, as can their absorption spectra.[12]

Halogen species adsorbed on various high surface area solids, such as zeolites,[18–22] silicas,[23] and Vycor glass[24] have been described in the literature in detail. It has been found that when halogen molecules are adsorbed on a surface their properties can significantly change and the reactivity of the halogen can significantly increase.[24] Risbood et al.[18] reported selective bromination of a side-chain double bond by bromine preadsorbed on a zeolite. It has also been reported that bromine adsorbed on zeolites is more chemically reactive than gas-phase bromine as a result of reduced molecular force constants.[19,20]

The advantage of using different nanosized metal oxides for adsorption of halogen and interhalogen is the varying strength of adsorption capability of the metal oxides. This could lead to the ability to fine-tune the final product to

* Corresponding author. E-mail: kenjk@ksu.edu.
[†] Kansas State University.
[‡] University of California at Santa Barbara.

(1) Ranjit, K. T.; Medine, G.; Jeevanandam, P.; Martyanov, I. N.; Klabunde, K. J. *Environ. Catal.* **2005**, 391–420.
(2) Demydov, D.; Klabunde, K. J. *NATO Sci. Ser., II: Mathematics, Physics and Chemistry* **2005**, *204*, 237–330.
(3) Martin, M. E.; Narske, R. M.; Klabunde, K. J. *Microporous Mesoporous Mater.* **2005**, *83*, 47–50.
(4) Klabunde, K. J.; Medine, G.; Bedilo, A.; Stoimenov, P.; Heroux, D. *ACS Symp. Ser.* **2005**, *890*, 272–276.
(5) Jeevanandam, P.; Klabunde, K. J.; Tetzler, S. H. *Microporous Mesoporous Mater.* **2005**, *79*, 101–110.
(6) Medine, G. M.; Zaikovski, V.; Klabunde, K. J. *J. Mater. Chem.* **2004**, *14*, 757–763.
(7) Carnes, C. L.; Klabunde, K. J. *J. Mol. Catal. A: Chem.* **2003**, *194*, 227–236.
(8) Stoimenov, P. K.; Zaikovski, V.; Klabunde, K. J. *J. Am. Chem. Soc.* **2003**, *125*, 12907–12913.
(9) Stoimenov, P. K.; Klinger, R. L.; Marchin, G. L.; Klabunde, K. J. *Langmuir* **2002**, *18*, 6679–6686.
(10) Koper, O. B.; Klabunde, J. S.; Marchin, G. L.; Klabunde, K. J.; Stoimenov, P. K.; Bohra, L. *Curr. Microbiol.* **2002**, *44*, 49–55.
(11) Sun, N.; Klabunde, K. J. *J. Am. Chem. Soc.* **1999**, *121*, 5587–5588.
(12) Jiang, X.-P.; Shapiro, M.; Brumer, P. *J. Chem. Phys.* **1996**, *105*, 3479–3485.
(13) Sadley, A. J. *J. Chem. Phys.* **1992**, *96*, 2048–2053.
(14) McCarthy, M. I.; Gerber, R. B. *J. Chem. Phys.* **1990**, *93*, 887–893.
(15) Kolodney, E.; Amirav, A.; Elber, R.; Gerber, R. B. *Chem. Phys. Lett.* **1984**, *111*, 366–371.
(16) Gerber, R. B.; Amirav, A. *J. Phys. Chem.* **1986**, *90*, 4483–4491.
(17) McCarthy, M. I.; Gerber, R. B.; Shapiro, M. *J. Chem. Phys.* **1990**, *92*, 7708–7715.
(18) Risbood, P. A.; Ruthven, D. M. *J. Am. Chem. Soc.* **1978**, *100*, 4919–4921.
(19) Cooney, R. P.; Tsai, P. *J. Raman Spectrosc.* **1979**, *8*, 195–198.
(20) Tsai, P.; Cooney, R. P. *J. Raman Spectrosc.* **1979**, *8*, 236–238.
(21) Rubim, J. C.; Sala, O. *J. Raman Spectrosc.* **1980**, *9*, 155–156.
(22) Rubim, J. C.; Sala, O. *J. Raman Spectrosc.* **1981**, *11*, 320–321.
(23) Nagasao, T.; Yamada, H. *J. Raman Spectrosc.* **1975**, *3*, 153–160.
(24) Favre, P.; Jayasooriya, U. A.; Powell, D. B. *J. Raman Spectrosc.* **1987**, *18*, 133–135.

10.1021/cm8000927 CCC: $40.75
Published on Web 04/22/2008

display the properties necessary for the desired application. For example, using these adducts as a safe way to store halogen and interhalogens would require a metal oxide with the capability to hold on to the halogen/interhalogen tightly for long periods of time, whereas in the use of these adducts as biocides, one could imagine using a metal oxide that only temporarily retains the halogen and then can release it to act as an oxidizer during contact with the bacterial cell. Stoimenov et al. have previously reported the use of nanosized halogen magnesium oxide adducts as biocides[8–10] and have stated that they are stable for several months.[8] This new class of materials have the potential to become very potent biocides that could by far exceed currently used materials. While biocidal properties of nanomaterials of various forms have been studied, this kind of material has only recently been discovered, and much is still to be explored.

Here, we describe the preparation of halogen and interhalogen adducts from three different nanosized metal oxides, Al_2O_3, TiO_2, and CeO_2. The prepared materials were characterized by Raman, UV−vis, and X-ray photoelectron spectroscopies as well as thermogravimetric analysis. Their straightforward preparation and the ability to prepare large amounts of product should make them attractive for future applications. We propose to use the prepared metal oxide halogen and interhalogen adducts as agents against vegetative cells and spores but also against viruses, which will be published at a later date.

Experimental Procedures

Materials. All halogen and interhalogen compounds (chlorine, bromine, iodine, iodine monochloride, iodine monobromide, and iodine trichloride) were purchased from Aldrich and used without further purification. NanoActive (NA) TiO_2, NA-Al_2O_3 Plus, and NA-CeO_2 were purchased from NanoScale Corp. (www.nanoactive.com).

To remove any water and carbon dioxide adsorbed on the surface of the metal oxides, an activation step was applied prior to adsorption of halogen/interhalogen. The activation step consisted of gradual heating of the material in a Schlenk tube to 400 °C over 2 h and then maintaining this temperature for another 4 h, either under O_2 atmosphere (NA-TiO_2) or under dynamic vacuum (NA-Al_2O_3 Plus and NA-CeO_2). Before adsorption of halogen/interhalogen, the samples were allowed to cool to room temperature.

Preparation of Chlorine, Bromine, and Iodine Monochloride Adducts. The procedure was carried out as described in the literature[8] and is described below.

Freshly activated powders, about 10 g, were allowed to contact with chlorine gas, or in case of Br_2 and ICl, connected to a Schlenk tube containing liquid Br_2 or ICl. The difference in pressure between the atmosphere above the metal oxide and in the halogen source allowed the transfer of Cl_2 gas or Br_2 and ICl vapors to the Schlenk tube containing the metal oxide. During this step, the outlet to the vacuum line was closed. As the color of the atmosphere above the powder changed to green-yellow (chlorine) or brown-red (bromine or iodine monochloride), the connection was disengaged and the powder was well shaken to encourage maximum contact. Another dose of halogen was transferred when the atmosphere above the powder had cleared up. Halogen dosage continued until the atmosphere above the powder did not clear up and free halogen remained. The halogen container was then disconnected and the powder was again connected to the vacuum line and maintained until the pressure reached 50×10^{-3} Torr or below. This step took approximately 20 min and ensured the removal of excess halogen. The freshly prepared halogen adduct was transferred and stored in a glass vial with a Teflon-lined cap.

Preparation of Iodine, Iodine Monobromide, and Iodine Trichloride Adducts. Iodine, iodine monobromide, and iodine trichloride are all solids and not volatile enough to be transferred as vapors as in the procedure described previously. Instead, solid material was added directly to the activated powder, and the powder was well shaken. Upon adsorption, the powder changed color. Another dose of solid halogen particles was added to ensure complete adsorption. Persistence of free halogen particles was considered the saturation point, and once reached, the powder was connected to the vacuum line and retained under dynamic vacuum until the pressure reached 50×10^{-3} Torr or below. At this point, no free halogen or interhalogen particles remained. The iodine sample was further heated to 125 °C to ensure enough volatility to remove excess iodine. The freshly prepared halogen adduct was then transferred to a Teflon-lined cap glass vial.

Experimental Techniques. FT-Raman spectra were collected on a Nicolet Nexus 670 with a Raman module using a continuous Nd:YAG laser (1064 nm). Either a liquid nitrogen-cooled germanium or InGaAs detector within the range of 4000−100 cm^{-1} was used. The sample holder consists of a static glass cylindrical Raman cuvette, and the laser power used was between 0.2 and 0.65 W.

A Varian UV−vis–NIR spectrophotometer Cary 500 Scan instrument was used to record diffuse reflectance and UV−vis spectra. Teflon powder (polytetrafluoroethylene) was used as a diffuse reflectance reference.

Thermogravimetric analysis (TGA) was conducted on a Shimadzu TGA model TA-50, under He atmosphere.

Quantachrome NOVA-1200 was used to determine the surface area of the materials. The BET method using nitrogen adsorption was utilized.

XPS was recorded on a Kratos Axis Ultra spectrometer. Monochromatic Al radiation was used with 50 meV energy step increments and 1200 ms dwell time. The samples were pressed flat on a double sticky tape and imaged in a vacuum of 1×10^{-8} Torr or better.

Results and Discussion

A. Characterization of Halogen/Interhalogen Adducts. Several different techniques were used to characterize the different halogen and interhalogen adducts. The results are presented below in separate sections.

Specific Surface Area, Stability, Surface Concentration, and TGA. NA-Al_2O_3 Plus is an amorphous high surface area metal oxide. The material consists mainly of mesopores and is a weakly aggregated material. Its chemical reactivity is high, and it is very suitable for adsorption. Specific surface area for the starting NA-Al_2O_3 Plus was determined to ∼550 m^2/g. The activation procedure of the sample did not change the surface area significantly, and this high surface area, as well as many corners, edges, and defect sites present in the material, makes it an excellent candidate for adsorption of halogens.[11] These unique surface properties enhance the reactivity of the material, leading to new possibilities. Similar to NA-Al_2O_3 Plus, NA-TiO_2 is also an amorphous high surface area material. It is a weakly aggregated, porous material with excellent adsorption capacity and high chemical reactivity. Specific surface area for the starting NA-TiO_2 was

Table 1. Quantitative Results from Analysis of NA-Al_2O_3 Plus Adducts

material	halogen content wt % (TGA)	surface conc molecules/nm^2	color
NA-Al_2O_3/CI_2 Plus	14	2.5	white
NA-Al_2O_3/Br_2 Plus	15	1.2	yellow
NA-Al_2O_3/I_2 Plus	18	1.0	brown
NA-Al_2O_3/ICI Plus	35	3.6	red-brown
NA-Al_2O_3/IBr Plus	28	2.1	brown
NA-Al_2O_3/ICl_3 Plus	37	2.8	yellow-brown
NA-TiO_2/Cl_2	3	2.6	white
NA-TiO_2/Br_2	5	2.0	yellow
NA-TiO_2/I_2	13	3.6	dark brown
NA-TiO_2/ICI	19	8.7	red-brown
NA-TiO_2/IBr	15	5.1	brown
NA-TiO_2/ICl_3	12	3.5	yellow-brown
NA-CeO_2/Cl_2	2	3.5	pale yellow
NA-CeO_2/Br_2	3	2.3	yellow
NA-CeO_2/I_2	5	2.5	dark brown
NA-CeO_2/ICI	4	3.1	brown
NA-CeO_2/IBr	4	2.4	red-brown
NA-CeO_2/ICl_3	4	2.2	red-brown

determined to ~500 m^2/g, but after the activation step this high surface area decreased to ~100 m^2/g and the amorphous sample transformed into anatase TiO_2 with a crystallite size of approximately 15 nm. NA-CeO_2 is a crystalline material with a crystallite size less than 7 nm before the activation step. Specific surface area for the starting NA-CeO_2 was determined to ~50 m^2/g, and after the activation step the crystallite size increased to about 10 nm.

Table 1 shows the wt % adsorbed halogen for the prepared adducts; values up to 37% by weight have been obtained. The weight percent adsorbed halogen on the surface is in general lower for the NA-TiO_2 and NA-CeO_2 adducts than for those of NA-Al_2O_3 Plus. This can be explained in part by the significantly lower surface area of NA-TiO_2 and especially NA-CeO_2 as compared to that of NA-Al_2O_3 Plus. The lower molecular weight of TiO_2 (79.9 g/mol) as compared to Al_2O_3 (102.0 g/mol), as well as the lower wt % of halogen adsorbed on the metal oxide surface, allows the conclusion that NA-TiO_2 is not as good of an adsorbant as compared to NA-Al_2O_3 Plus. The NA-CeO_2 adducts retained much lower amounts of halogen/interhalogen as compared to the other two metal oxides. In addition to its much lower surface area, this can be explained by the much higher molar mass of NA-CeO_2 (172.1 g/mol) as compared to the two other metal oxides. During the adsorption process, it can be observed that the halogen is adsorbed very quickly on the cerium oxide surface and the stability of the prepared halogen adducts is very good, especially as compared to the NA-TiO_2 adducts.

In addition to the already mentioned nanosized metal oxides, their commercially available counterparts were also tested for adsorption of halogen. γ-Al_2O_3, α-Al_2O_3, anatase-TiO_2, rutile-TiO_2, and CeO_2 were allowed contact with bromine, but none of the materials adsorbed and retained any bromine, indicating the importance of surface structure and surface area of the adsorbant. The surface structure is believed to be of significance during the adsorption process. Stoimenov et al. reported that commercially available (CM)-MgO adsorbed and retained smaller amounts of halogen/interhalogen in comparison to nanosized MgO.[8] In addition, the obtained adducts possessed much stronger halogen smells and were not stable for as long as the adducts prepared from nanosized MgO. In our case, the commercially available counterparts of the metal oxides studied herein did not retain any bromine. We attribute this to be caused by their much lower surface area and less complex surface structures, including significantly fewer defect sites, edges, and apexes. The bulk phase is rather composed of low activity flat faces of the micrometer size.

The adducts prepared from NA-Al_2O_3 Plus, NA-TiO_2, and NA-CeO_2 are all fairly stable and can be safely stored in a vial for several months and then used. The adducts prepared from NA-Al_2O_3 Plus and NA-CeO_2 are more stable than those from NA-TiO_2. If the adducts were exposed to the ambient atmosphere, the adducts lost halogen over time. On the benchtop, the iodinated adducts were the most stable, taking more than 30 h for the iodine on the surface to dissipate in the case of NA-Al_2O_3/I_2 Plus. Several of the interhalogen adducts are also very stable, as expected because they are polar molecules and will interact strongly with the ionic metal oxide surface, whereas the brominated adducts were less stable. This coincides well with the thermogravimetric analysis data that showed that iodine was lost at a higher temperature than the interhalogen molecules (data not shown). NA-Al_2O_3/Br_2 Plus had lost most of its bromine already at 40 °C and was much less stable. Among the interhalogen adducts, NA-Al_2O_3/ICl Plus was the most stable, most likely due to the large dipole moment of the iodine monochloride molecule, leading to a very strong interaction with the ionic oxide surface.

Temperature effects could be of considerable importance in relation to the strength of adsorption and have been considered. During adsorption of the halogen/interhalogen on the three used metal oxides, no evolved heat was observed. In the report by Stoimenov et al.,[8] considerable heat was evolved upon adsorption on nanosized MgO, whereas much lower amounts of heat were observed in the case of micrometer-sized MgO. These results indicated a much stronger adsorption in the case of nanosized MgO versus the micrometer-sized MgO, and we therefore conclude the presence of a weaker adsorption of the halogen/interhalogen to the metal oxide surface in the case of NA-Al_2O_3 Plus, NA-TiO_2, and NA-CeO_2 as compared to nanosized MgO.

The calculated surface concentration of the adducts is shown in Table 1 and varies between 1.0 and 8.7 molecules/nm^2. These values are higher than those obtained by Stoimenov et al.[8] on nanosized MgO. The surface concentration for the NA-TiO_2 adducts is in general higher than that for the NA-Al_2O_3 Plus and NA-CeO_2, reaching 8.7 molecules/nm^2 for the ICl adduct.

UV−Vis Spectra Analysis. The nonpolar halogens and the polar interhalogen compounds investigated in this study all exhibit significant absorption in the UV−visible light range. Many of them have been explored in the gas phase and in different solvents, both polar and nonpolar.[25–33] During absorption of light, the halogen and interhalogen molecules

(25) Gillam, A. E.; Morton, R. A. *Proc. R. Soc. London* **1929**, *A124*, 604–616.

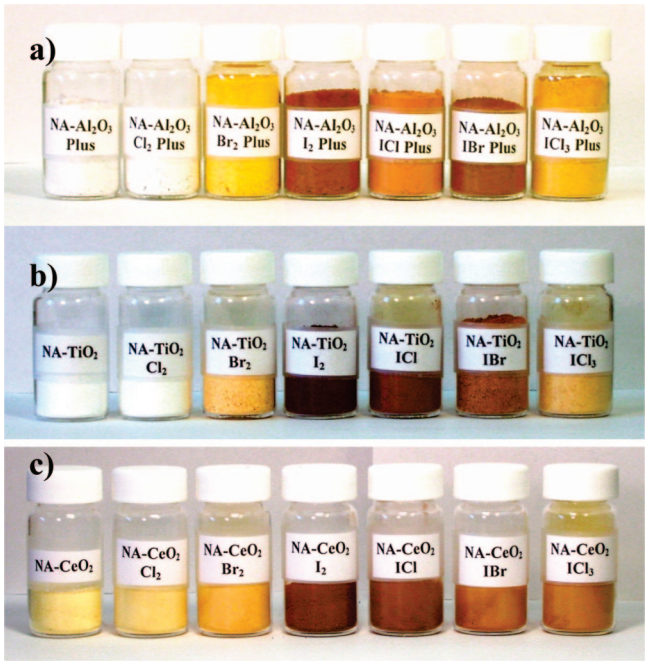

Figure 1. Photographs of halogen/interhalogen adducts of (a) NA-Al_2O_3 Plus; (b) NA-TiO_2; and (c) NA-CeO_2.

undergo several electronic transitions from the ground state to one or more of the excited electronic states, which leads to a number of broad bands in the UV−vis spectrum.[26,27,32] Several works in the literature have described theoretically and experimentally how different halogen and interhalogens, such as I_2, ICl, and IBr, interact with various surfaces, for example, with magnesium oxide, at different temperatures.[12,14–17] Very large molecule-surface energy transfer has been observed in the case of I_2 collision with the MgO surface.[15,16] Further, theoretical simulations indicate a change in orientation of the interhalogen molecule ICl at the surface, at temperatures ranging from below 150 K and above 350 K.[14] At lower temperatures, the ICl molecule occupies a single orientational site, whereas at higher temperatures the molecule hops between two different orientational sites on the surface. Jiang et al.[12] have developed a model for computing the absorption spectrum of diatomic molecules adsorbed on a nonzero temperature surface in hope that it will yield valuable information about molecule–surface interactions. Several works indicate that the electronic structure of the molecule and hence their absorption spectra can be changed significantly upon adsorption.[12,14,17]

A photograph of the prepared adducts can be seen in Figure 1. NA-Al_2O_3 Plus is a white powder with essentially no absorbance in the 200−800 nm range. Similarly, NA-Al_2O_3/Cl_2 Plus is a nearly white powder with a diffuse reflectance spectrum identical to that of NA-Al_2O_3 Plus. Further, NA-TiO_2 is a white powder with absorbance in the 200−400 nm range, but no absorbance in the 400−800 nm range. Similarly, NA-TiO_2/Cl_2 is a nearly white powder with a diffuse reflectance spectrum matching well with that of NA-TiO_2. NA-CeO_2, however, has a pale yellow color and displays absorbance in the 200−500 nm range, as reported in the literature,[34–36] with a peak position at ∼350 nm. NA-CeO_2/Cl_2 has a diffuse reflectance spectrum coinciding with NA-CeO_2. It can be observed clearly in Figure that the chlorinated samples appear nearly identical to the "naked" metal oxides.

NA-Al_2O_3/Br_2 Plus is yellow in color and shows significant absorption with a peak position at 275 nm and a shoulder at 390 nm (Figure 2a). These values can be compared to Br_2 dissolved in CCl_4 with peak positions at 255 and 440 nm. Further, in the case of NA-TiO_2/Br_2, also a yellow colored powder, the absorbance spectrum shows a shoulder around 340 nm (Figure 2a). NA-CeO_2/Br_2 has an absorbance spectrum that is similar to that of NA-CeO_2 but with a slightly wider absorption range (Figure 2a). The spectrum is very different from that of Br_2 dissolved in CCl_4.

Iodine dissolved in CCl_4 has two distinct peaks at 260 and 516 nm, whereas NA-Al_2O_3/I_2 Plus has a broader absorption spectrum with peak positions at 294 and 373 nm (Figure 2b). NA-TiO_2/I_2 has a broader absorption spectrum as compared to NA-TiO_2 with a peak position at 500 nm (Figure 2b). Similarly, NA-CeO_2/I_2 has a very broad absorption spectrum but with no specific features (Figure 2b).

ICl in CCl_4 has two intense peaks at 250 and 460 nm, while NA-Al_2O_3/ICl Plus has a wider band with peak positions at 229 and 475 nm and a shoulder at approximately 345 nm (Figure 2c). NA-TiO_2/ICl has a wide band with peak positions at 330 and 470 nm (Figure 2c), whereas NA-CeO_2/ICl has a wider band with peak positions at 350 and 520 nm (Figure 2c).

The diffuse reflectance spectrum of NA-Al_2O_3/IBr is less distinct than IBr dissolved in CCl_4, displaying a peak position at 306 nm and a broad shoulder around 500 nm (Figure 2d). The diffuse reflectance spectrum of NA-TiO_2/IBr is broad with a decreasing intensity with increasing wavelength. Its shoulder at 500 nm coincides well with the peak of IBr itself (Figure 2d). The spectrum of NA-CeO_2/IBr similarly displays a decreasing intensity with increasing wavelength with a peak position at 350 nm and a shoulder at 475 nm. Its shoulder coincides well with the peak of IBr itself (Figure 2d).

The spectrum of NA-Al_2O_3/ICl_3 Plus has two peaks at 238 and 345 nm and is very similar in appearance to the spectrum of NA-Al_2O_3/IBr Plus (Figure 2e). The diffuse reflectance spectrum of NA-TiO_2/ICl_3 is likewise similar in appearance to that of NA-TiO_2/IBr, but with a slightly weaker absorbance in the range 400−800 nm (Figure 2e). The diffuse reflectance spectrum of NA-CeO_2/ICl_3 is also similar in appearance to that of the IBr adduct, with a peak position at 350 nm, but with the shoulder at a higher wavelength (Figure 2e).

(26) Acton, A. P.; Aickin, R. G.; Bayliss, N. S. *J. Chem. Phys.* **1936**, *4*, 474–479.
(27) Gray, R. I.; Luckett, K. M.; Tellinghuisen, J. *J. Phys. Chem. A* **2001**, *105*, 11183–11191.
(28) Seery, D. J.; Britton, D. *J. Phys. Chem.* **1964**, *68*, 2263–2266.
(29) Wren, J. C.; Paquette, J.; Sunder, S.; Ford, B. L. *Can. J. Chem.* **1986**, *64*, 2284–2296.
(30) Gibson, G. E.; Ramsperger, H. C. *Phys. Rev.* **1927**, *30*, 598–607.
(31) Binder, J. L. *Phys. Rev.* **1938**, *54*, 114–117.
(32) Nebeker, E. B.; Pings, C. J. *J. Phys. Chem.* **1965**, *69*, 2483–2484.
(33) Rogers, L. J.; Ashfold, M. N. R.; Matsumi, Y.; Kawasaki, M.; Whitaker, B. J. *Chem. Phys. Lett.* **1996**, *258*, 159–163.
(34) Sathyamurthy, S.; Leonard, K. J.; Dabestani, R. T.; Paranthaman, M. P. *Nanotechnology* **2005**, *16*, 1960–1964.
(35) Ho, C.; Yu, J. C.; Kwong, T.; Mak, A. C.; Lai, S. *Chem. Mater.* **2005**, *17*, 4514–4522.
(36) Yan, B.; Zhao, W. *J. Adv. Mater* **2006M**, 44–47.

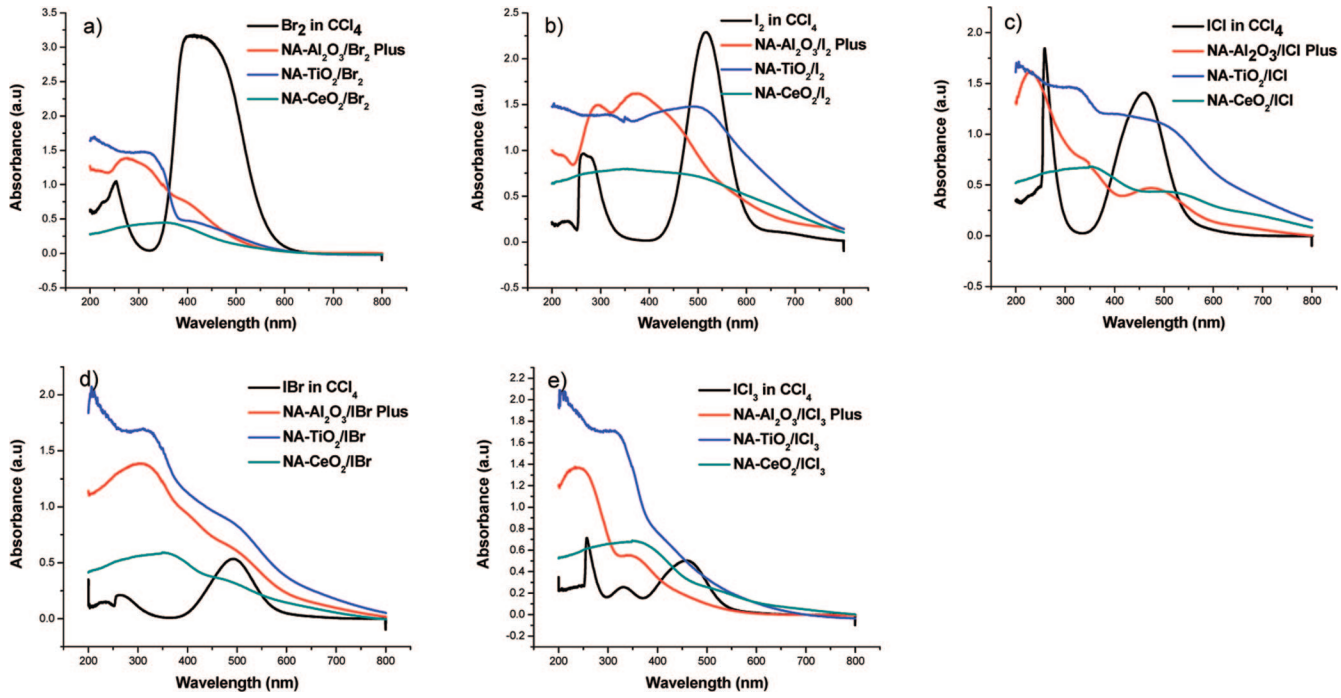

Figure 2. UV−vis and diffuse reflectance spectra of (a) Br_2 adducts and Br_2 in CCl_4; (b) I_2 adducts and I_2 in CCl_4; (c) ICl adducts and ICl in CCl_4; (d) IBr adducts and IBr in CCl_4; and (e) ICl_3 adducts and ICl_3 in CCl_4. These spectra show that the n → π^* transition in the free halogens is significantly blue-shifted, especially for the Al_2O_3 adducts.

We have observed significant changes in the electronic transitions in several of the prepared adducts, indicating changes in reactivity of the halogenated materials. In general, the adducts prepared from NA-CeO_2 display broader absorbance spectra without specific characteristic, whereas the other two metal oxide adducts display more distinct absorption peaks.

Raman Spectra Analysis. The halogens and interhalogens have been extensively studied and their Raman spectra recorded both in the gas and in the condensed phase.[37–49] Both Raman and infrared spectroscopies have been used frequently in the past to study the formation and strength of the interaction between different donors and acceptors. Several of the halogens and interhalogens have been investigated,[50–54] but other molecules have been of interest as well.[55,56] Raman and infrared spectroscopies are very useful in the detection of small changes in molecules. Raman spectroscopy is suitable for the study of these halogen and interhalogen changes, especially as even the nonpolar halogen molecules vibration are only Raman active, whereas they are not infrared active.

The nature of the interaction that takes place between the halogen/interhalogen with the metal oxide surface is of considerable interest. Stoimenov et al.[8] reported halogen/interhalogen adsorbed on nanosized magnesium oxide and concluded that a strained halogen–halogen bond existed, causing a frequency shift of the halogen vibration to a lower wavenumber in the Raman spectrum. Actually, two different possibilities of adsorption have been suggested[8] and are described in short below:

Case 1: This involves chemisorption without polarization or bond cleavage of the halogen/interhalogen. This would cause a lengthening and weakening of the halogen/interhalogen bond and hence a lowering of the energy of vibration of the halogen itself in the Raman spectrum. One should expect to see the vibration of the halogen/interhalogen moiety as well as the metal oxide lattice vibration in the Raman spectrum if this occurs. Klaboe[52] has described a possible intensity variation of the lattice vibrations in the Raman spectrum during the interaction with halogens. Cooney et al.[19] have reported that the shift of the halogen vibration can vary significantly depending upon the strength of adsorption.

Case 2: The polarization of the halogen/interhalogen molecule is stabilized by the dipoles of the metal oxide surface (metal cations and oxygen anions), leading to bond breakage and further formation of new bonds causing disproportionation of the surface. This would cause new

(37) Stammreich, H. *Phys. Rev.* **1950**, *78*, 79–80.
(38) Stammreich, H.; Forneris, R. *J. Chem. Phys.* **1954**, *22*, 1624.
(39) Stammreich, H.; Forneris, R.; Tavares, Y. *Spectrochim. Acta* **1961**, *17*, 1173–1184.
(40) Anderson, A.; Sun, T. S. *Chem. Phys. Lett.* **1970**, *6*, 611–616.
(41) Holzer, W.; Murphy, W. F.; Bernstein, H. J. *J. Chem. Phys.* **1970**, *52*, 399–407.
(42) Cahill, J. E.; Leroi, G. E. *J. Chem. Phys.* **1969**, *51*, 4514–4519.
(43) Melveger, A. J.; Brasch, J. M.; Lippincott, E. R. *Mater. Res. Bull.* **1969**, *4*, 515–523.
(44) Suzuki, M.; Yokoyama, T.; Ito, M. *J. Chem. Phys.* **1969**, *51*, 1929–1931.
(45) Suzuki, M.; Yokoyama, T.; Ito, M. *J. Chem. Phys.* **1969**, *50*, 3392–3398.
(46) Anthonsen, J. W. *Spectrochim. Acta* **1976**, *32A*, 963–970.
(47) Stammreich, H.; Kawano, Y. *Spectrochim. Acta.* **1968**, *24A*, 899–904.
(48) Brooks, W. V. F.; Crawford, B., Jr *J. Chem. Phys.* **1955**, *23*, 363–365.
(49) Herzberg, G. *Spectra of Diatomic Molecules*, 2nd ed.; D. Van Nostrand, Co., Inc.: New York, 1950.
(50) Person, W. B.; Humphrey, R. E.; Deskin, W. A.; Popov, A. I. *J. Am. Chem. Soc.* **1958**, *80*, 2049–2053.
(51) Person, W. B.; Erickson, R. E.; Buckles, R. E. *J. Am. Chem. Soc.* **1960**, *82*, 29–34.

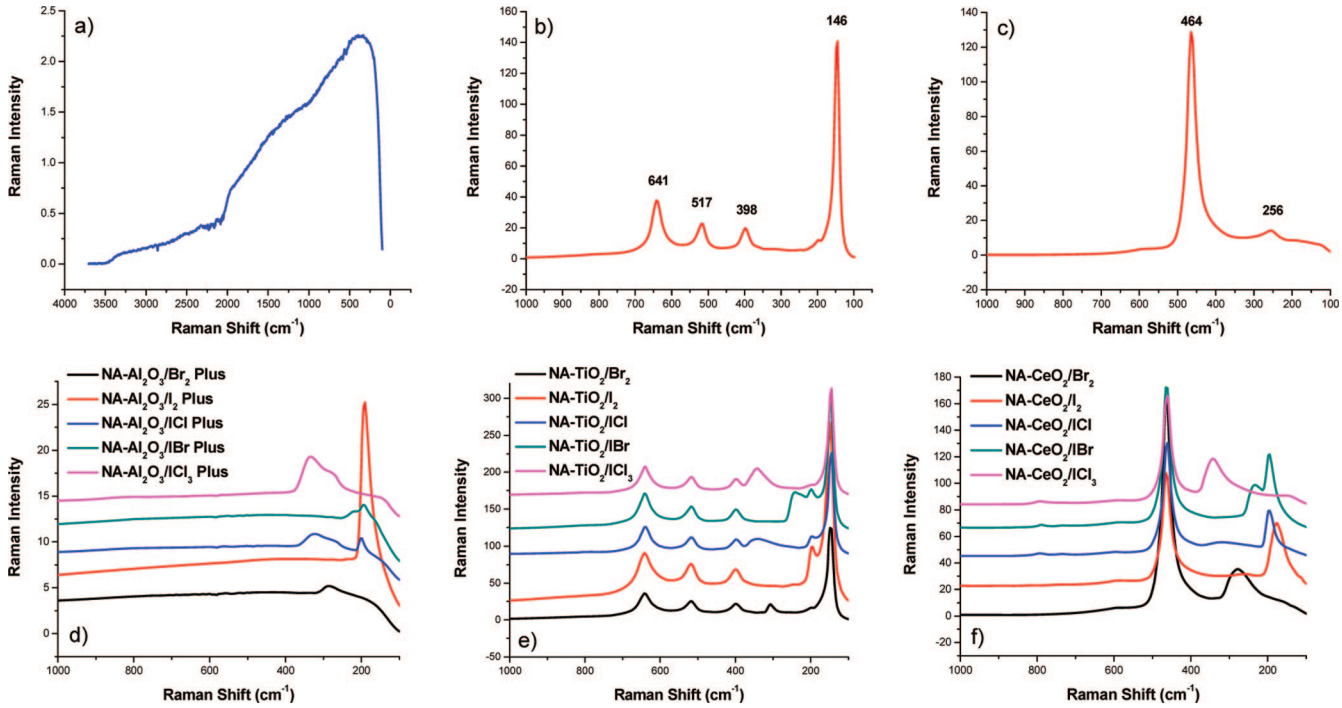

Figure 3. Raman spectra of (a) NA-Al_2O_3 Plus; (b) NA-TiO_2; (c) NA-CeO_2; (d) NA-Al_2O_3 Plus adducts; (e) NA-TiO_2 adducts; and (f) NA-CeO_2 adducts. See text for discussion. Generally, shifted halogen–halogen bonds are observable, indicating that adsorption on the nanooxide is strong, but not dissociative.

species on the surface, such as M–X(Y) and/or O–X(Y), where M is the metal and X, Y = Cl, Br, I. These new species would then lead to the appearance of new bands that are allowed in the Raman spectrum.

The Raman spectrum of activated NA-Al_2O_3 Plus shows a broad peak with a peak position at 376 cm^{-1} (Figure 3a). The chlorinated adduct shows a similar spectrum (not shown), with no distinct peak for the chlorine stretch. One possible explanation to the absence of the Cl_2 peak includes the fact that the Raman intensity is directly related to the degree of polarizable ability of the Raman active molecule. Cl_2 is less polarizable than Br_2 and even more so than I_2, leading to a less intense peak, or absence of the peak. In addition, the amount of Cl_2 present is lower than the amount of Br_2 and I_2 in all of the prepared adducts, further explaining the absence of a chlorine peak. Stoimenov et al. reported a Cl_2 peak at 491.7 cm^{-1} for the chlorinated adduct of nanosized MgO; however, the intensity of the peak was weak.[8] The frequency for chlorine in the gas phase has been determined to 557 cm^{-1}.[39] The Raman spectrum of activated NA-TiO_2 clearly indicates that the metal oxide is in the anatase phase, as supported by the literature,[57–59] with peaks at 640.9, 517.3, 398.2, and 146.1 cm^{-1} (Figure 3b). The chlorinated adduct again shows no chlorine peak. The Raman spectrum of activated NA-CeO_2 shows one strong peak at 463.7 cm^{-1} and one smaller peak at 256.2 cm^{-1} (Figure 3c). The obtained peak values match up well to the findings of Shyu et al.[60] with reported values of a strong peak at 465 cm^{-1}, corresponding to the F_{2g} Raman active mode that is characteristic of fluorite structured materials, as well as a smaller, weaker band at 265 cm^{-1}. The small crystallite sizes of the NA-CeO_2 might be the explanation for the slightly lower wavenumbers, as compared to the literature values.[60] As with the chlorinated adducts of NA-Al_2O_3 Plus and NA-TiO_2, the chlorinated adduct of NA-CeO_2 does not have a Raman spectrum different from that of the metal oxide itself.

NA-Al_2O_3/Br_2 Plus shows an intense peak at 286 cm^{-1}, which can be compared to Br_2 in the gas phase with a peak position at 313.9 cm^{-1} (Figure 3d).[8,41] This shift of 28 cm^{-1} is significant and can be attributed to significant weakening of the Br−Br bond, leading to a lowering of the energy of vibration. There is no spectral evidence indicating formation of Br_3^-, which has a frequency value reported between 160 and 170 cm^{-1}[1,22,24,52,54,61,62] or of Br_5^- with a Raman shift of 250 cm^{-1}.[61] Several oxygen-containing bromine compounds, such as BrO_x^- have been discussed in the literature.[61,63–65] The reported values for BrO^-, BrO_2^-, BrO_3^-,

(52) Klaboe, P. *J. Am. Chem. Soc.* **1967**, *89*, 3667–3676.
(53) Kimel′fel′d, Ja. M.; Mostovoy, A. B.; Mostovaja, L. M. *Chem. Phys. Lett.* **1975**, *33*, 114–117.
(54) Loo, B. H.; Lee, Y. G. *J. Phys. Chem.* **1984**, *88*, 706–709.
(55) Person, W. B.; Humphrey, R. E.; Popov, A. I. *J. Am. Chem. Soc.* **1959**, *81*, 273–277.
(56) Heaviside, J.; Hendra, P. J.; Tsai, P.; Cooney, R. P. *J. Chem. Soc., Faraday Trans. 1* **1978**, *74*, 2542–2549.
(57) Iida, Y.; Furukawa, M.; Aoki, T.; Sakai, S. *Appl. Spectrosc.* **1998**, *52*, 673–678.
(58) Niilisk, A.; Moopel, M.; Pärs, M.; Sildos, I.; Jantson, T.; Avarmaa, T.; Jaaniso, R.; Aarik, J. *Cent. Eur. Sci. J. Phys.* **2006**, *4*, 105–116.
(59) Domae, M.; Tani, J.-I.; Fujiwara, K.; Katsumura, Y. *J. Nucl. Sci. Technol.* **2006**, *43*, 675–680.
(60) Shyu, J. Z.; Weber, W. H.; Gandhi, H. S. *J. Phys. Chem.* **1988**, *92*, 4964–4970.
(61) Evans, J. C.; Lo, G. Y.-S. *Inorg. Chem.* **1967**, *6*, 1483–1486.
(62) Person, W. B.; Anderson, G. R.; Fordemwalt, J. N.; Stammreich, H.; Forneris, R. *J. Chem. Phys.* **1961**, *35*, 908–914.
(63) Brown, L. C.; Begun, G. M.; Boyd, G. E. *J. Am. Chem. Soc.* **1969**, *91*, 2250–2254.
(64) Chantry, G. W.; Plane, R. A. *J. Chem. Phys.* **1961**, *34*, 1268–1271.
(65) Levason, W.; Ogden, J. S.; Spicer, M. D.; Young, N. A. *J. Chem. Soc., Dalton Trans.: Inorg. Chem.* **1990**, *1*, 349–353.

and BrO_4^- are all higher than 400 cm^{-1} and hence at a much higher wavenumber than the observed Raman peak in the spectrum of NA-Al_2O_3/Br_2 Plus. Beattie et al.[66] have reported Raman values for aluminum trihalides in the gas phase at different temperatures. The observed Raman band of the NA-Al_2O_3/Br_2 Plus adduct at 286 cm^{-1} does not coincide with the reported frequency bands of $AlBr_3$ at 360, 228, and 93 cm^{-1}. We therefore exclude bond breakage and formation of new surface species, or at least assume that they are formed to a negligible extent. The brominated adduct of NA-TiO_2 shows a peak in the Raman spectrum at 307 cm^{-1}, which gives a small downshift of 7 cm^{-1} (Figure 3e). The liquid and vapor-phase Raman spectra of titanium tetrabromide have been reported by Clark et al.[67] The strongest frequency band appears at 231.5 cm^{-1} (vapor-phase) or 229.5 cm^{-1} (liquid phase), neither of which appear present in the Raman spectrum of NA-TiO_2/Br_2, reported here. NA-CeO_2 has a Raman peak corresponding to Br_2 at 279 cm^{-1} (Figure 3f), which gives a 35 cm^{-1} lowering of the Br_2 peak. To our knowledge, there are no reports in the literature of Raman bands for cerium tetrabromide, and because there is no evidence of the formation of oxygen-containing species, we assume no formation of $CeBr_4$, or it occurs to a very small extent.

I_2 itself has a Raman peak at 213 cm^{-1},[39,41,46] and NA-Al_2O_3/I_2 Plus has a peak at 192 cm^{-1}, corresponding to a shift of 21 cm^{-1}(Figure 3d). Reported frequency values for I_3^- are in the range of 110−120 cm^{-1},[22,24,39,68] and there is no evidence for such a species in the Raman spectrum of the I_2 adduct. Kiefer et al. reported the Raman band for I_5^-[68] at 160 cm^{-1}, which is also lower than the observed frequency of our adduct. Oxygen-containing species, such as IO_3^-, IO_4^-, and IO_6^-,[63,64] all have Raman bands much higher than that observed, and the formation of such compounds is excluded or it is assumed that it occurs only to a small extent. AlI_3 has been investigated using Raman spectroscopy by Beattie et al.,[66] and two bands at 64 and 156 cm^{-1} are reported, in neither of which is found evidence for NA-Al_2O_3/I_2 Plus. The iodinated adduct of NA-TiO_2 has a small shift of 17 cm^{-1} with NA-TiO_2/I_2 displaying a Raman peak at 196 cm^{-1} (Figure 3d). Several works in the literature have reported the Raman spectrum of titanium tetraiodide.[67,69,70] Its spectrum has been obtained as a solid[69] or from TiI_4 dissolved in cyclohexane[67,69,70] with the most intense peak appearing around 160−162 cm^{-1}. We therefore exclude the formation of this species as well. A slightly stronger peak, at 177 cm^{-1}, was observed for NA-CeO_2/I_2, giving a shift of 36 cm^{-1} (Figure 3f). To the best of our knowledge, no reports exist containing the Raman spectrum of cerium tetraiodide.

ICl in the gas phase has an intense Raman peak at 381.5 cm^{-1},[39,41,48,49] whereas NA-Al_2O_3/ICl Plus has two Raman peaks, one at 200 cm^{-1} and one broader peak at 325 cm^{-1} (Figure 3d). A couple of works in the literature[8,39] have reported large frequency shifts of the ICl stretch during interaction with other surfaces. ICl is a polar molecule, possibly causing a strong interaction with the ionic metal oxide surface, leading to a large Raman shift. Isotopic splitting of the halogen peak has been discussed in the literature frequently as a cause for several peaks,[38–41,43–46,50] but these two peaks do not arise from an isotope effect because the frequency difference is much too large. Several works in the literature have reported Raman bands for ICl_2^- and ICl_4^- as 254−278 cm^{-1},[39,52,62,71] and 288 cm^{-1},[72] respectively, in which range we do not see any peaks in the Raman spectrum of the ICl adduct. One explanation for the two values would be that the value at 200 cm^{-1} is due to I_2 on NA-Al_2O_3 Plus and the value at 325 cm^{-1} is due to ICl on the surface of NA-Al_2O_3 Plus, leading to a downshift of 56.5 cm^{-1}. Calder et al.[73] reported that solid interhalogen, such as ICl, has not only ICl in its vapor phase but also I_2 and Cl_2. In addition, Nagasao et al. have reported that during adsorption of ICl on silica,[23] the Raman spectrum shows decomposition of ICl at the silica surface resulting in iodine on the surface. Partial decomposition upon adsorption has also been speculated by McCarthy et al., where IBr on the surface of MgO results in I_2 and Br_2 on the surface.[17] NA-TiO_2/ICl also displays two peaks, one at 340 and one at 196 cm^{-1} (Figure 3e). Using the same reasoning, the peak at 196 cm^{-1} can be explained by I_2 adsorbed on the surface, whereas the peak at 340 cm^{-1} corresponds to ICl on the surface, which would mean a downshift of 41.5 cm^{-1} as compared to ICl itself. NA-CeO_2/ICl displays a strong peak at 196 cm^{-1} and one small peak at 320 cm^{-1} (Figure 3f). The ICl peak at 320 cm^{-1} leads to a downshift of 61.5 cm^{-1}, which is realistic, as ICl is a polar molecule, leading to a strong interaction with the ionic surface of the metal oxide.

The Raman band for IBr in the gas phase has been reported at 267 cm^{-1},[46] while NA-Al_2O_3/IBr Plus has one peak at 194 cm^{-1}, and one peak at 218 cm^{-1} (Figure 3d). The peak at 194 cm^{-1} lies very close to the one resulting from NA-Al_2O_3/I_2 Plus and is most likely caused by the presence of I_2 and Br_2 in addition to IBr upon adsorption, resulting in adsorption of I_2 as well as IBr. In addition, the I_2 peak can be caused by partial decomposition of IBr to I_2 upon adsorption. The frequency downshift of 49 cm^{-1} of the IBr molecule seems reasonable in comparison to the previously discussed ICl shift. IBr is slightly less polar than ICl and should hence interact less strongly with the ionic surface of the metal oxide, leading to a smaller downshift. NA-TiO_2/IBr also displays two peaks, one at 241 and one at 199 cm^{-1} (Figure 3e). As compared to IBr in the gas phase at 267 cm^{-1},[46] this is a downshift of 26 cm^{-1} for the observed 241 cm^{-1} value. The second peak at 199 cm^{-1} can again be attributed to I_2 on the surface. Similarly NA-CeO_2/IBr displays two peaks: one larger resulting from I_2 at 196 cm^{-1}

(66) Beattie, I. R.; Horder, J. R. *J. Chem. Soc.* **1969**, *17*, 2655–2659.
(67) Clark, R. J. H.; Hunter, B. K.; Rippon, D. M. *Inorg. Chem.* **1972**, *11*, 56–61.
(68) Kiefer, W.; Bernstein, H. J. *Chem. Phys. Lett.* **1972**, *16*, 5–9.
(69) Clark, R. J. H.; Mitchell, P. D. *J. Am. Chem. Soc.* **1973**, *95*, 8300–8304.
(70) Clark, R. J. H.; Willis, C. J. *J. Chem. Soc. A* **1971**, *6*, 838–840.
(71) Maki, A. G.; Forneris, R. *Spectrochim. Acta* **1967**, *23A*, 867–880.
(72) Stammreich, H.; Forneris, R. *Spectrochim. Acta* **1960**, *16*, 363–367.
(73) Calder, G. V.; Giauque, W. F. *J. Phys. Chem.* **1965**, *69*, 2443–2452.

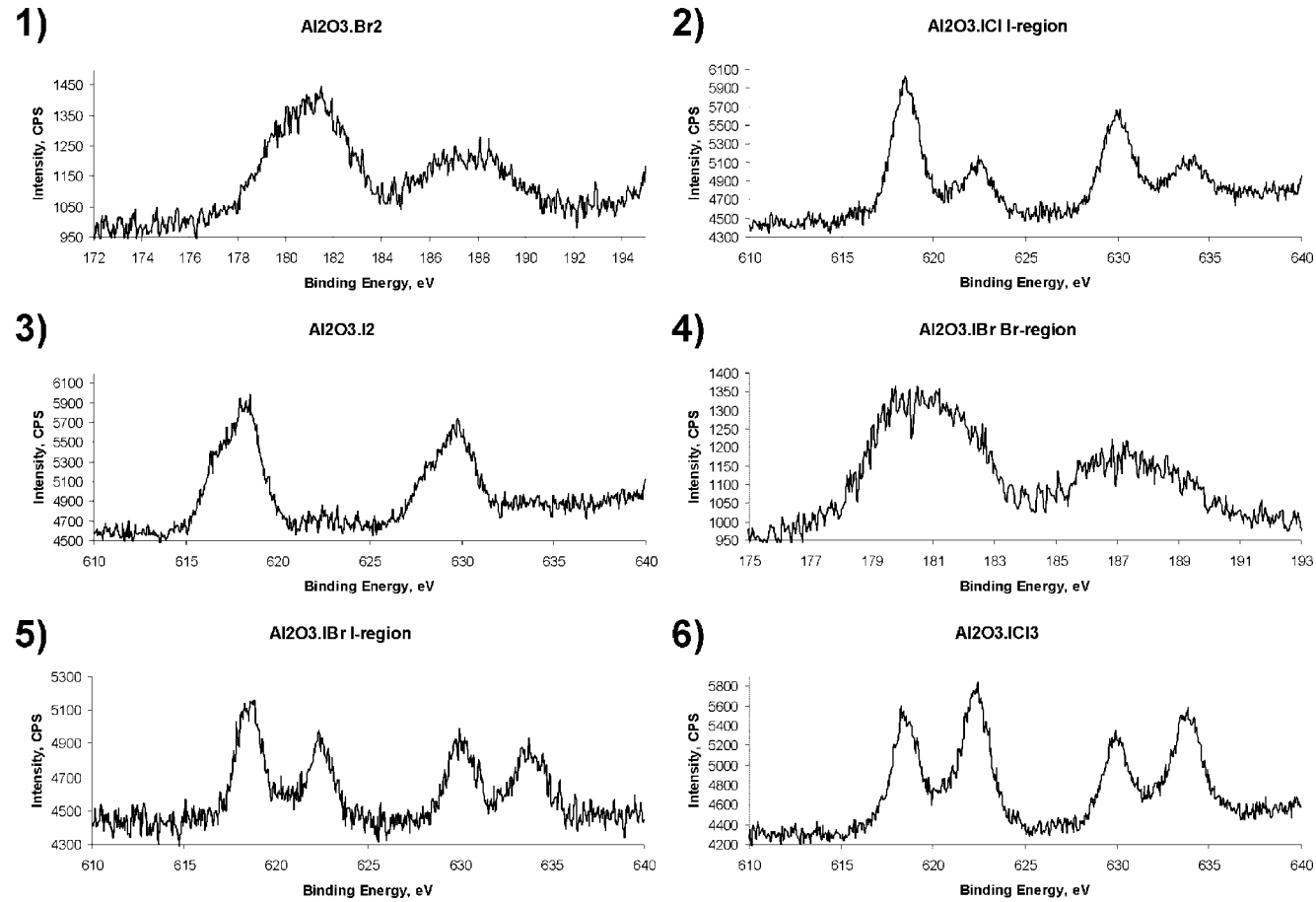

Figure 4. XPS spectra of NA-Al_2O_3 halogen and interhalogen adsorbates. (1) $Al_2O_3 \cdot Br_2$ ($3p^{3/2}$ and $3p^{1/2}$); (2) $Al_2O_3 \cdot ICl$ (iodine region, $3d^{5/2}$ and $3d^{3/2}$); (3) $Al_2O_3 \cdot I_2$ ($3d^{5/2}$ and $3d^{3/2}$); (4) $Al_2O_3 \cdot IBr$ (Br region, $3p^{3/2}$ and $3p^{1/2}$); (5) $Al_2O_3 \cdot IBr$ (iodine region, $3d^{5/2}$ and $3d^{3/2}$); (6) $Al_2O_3 \cdot ICl_3$ (iodine region, $3d^{5/2}$ and $3d^{3/2}$). Elemental halogens in the adsorbed state are observable, even under high vacuum, except for chlorine.

and one smaller resulting from IBr at 233 cm^{-1} (Figure 3f). The downshift of 34 cm^{-1} for the IBr moiety is reasonable as compared to the larger ICl shift for NA-CeO_2/ICl of 61.5 cm^{-1}.

The Raman spectrum of solid ICl_3 consists of several peaks:[8,47] two intense peaks at 343.2 and 312.3 cm^{-1}, followed by several very small peaks of values 198.6, 142.6, and 117.6 cm^{-1}. The Raman spectrum of NA-Al_2O_3/ICl_3 Plus, however, is very different, and it displays one peak at 334 cm^{-1} and one shoulder at 280 cm^{-1} (Figure 3d). It is possible that the three small peaks of ICl_3 are lost in the broad background spectra of NA-Al_2O_3 Plus, but a chemical reaction of some sort can not be completely ruled out. The surface is very reactive, and a variety of reactions might have taken place. NA-TiO_2/ICl_3 displays one peak at 342 cm^{-1}, almost exactly coinciding with the most intense peak of ICl_3 itself at 343.2 cm^{-1} (Figure 3e). It is again possible that the less intense peaks of ICl_3 are hidden by the metal oxide background moiety, including the very intense anatase peak at 146.1 cm^{-1} and the shoulder at slightly higher wavenumber. The very small downshift of 1.2 cm^{-1} most likely means that the halogen is retained in the pore structure or adsorbed very loosely on the surface. It does not seem likely that either $TiCl_4$ or TiI_4 has formed; their Raman bands have been reported in the literature as 389 and 162 cm^{-1}, respectively.[67] NA-CeO_2/ICl_3 has a peak that also almost completely coincides with the strongest peak of ICl_3 itself, at 343 cm^{-1} (Figure 3f), again indicating that the interhalogen might be retained in the pore structure of the metal oxide or adsorbed only loosely on the surface. The loss of the other peaks could be due to the low threshold of sensitivity.

X-ray Photoelectron Spectroscopy, XPS, Analysis. The XPS analysis was conducted on the NA-Al_2O_3 Plus adducts to confirm the presence of halogen on the surface of the materials and their chemical state. Halogens/interhalogens were observed in all cases except the NA-Al_2O_3/Cl_2 Plus adduct, when the observed spectrum was identical to that of pure NA-Al_2O_3 Plus (data not shown). However, this observation is attributed to the volatility induced by the local heating by the intensive X-ray beam. This hypothesis is supported by the fact that asimilar effect was induced with the bromine adduct when long acquisition time was used. Thus, relatively short acquisition times were used for all samples to avoid X-ray-induced desorption and decomposition of the fairly unstable interhalogen compounds. The bromine and iodine samples have peak locations as expected for free elements (Figure 4(1) and (3)),[74] consisting of a set of two peaks in each case. Peaks confirming salt formation were not observed in any case, including the pure chlorine adsorbate. For all interhalogens, four peaks was observed: one set of two peaks has higher binding energy corresponding

(74) Ishihara, M.; Okumura, J.; Yamaguchi, K. *J. Polym. Sci.* **1996**, *34*, 587–590.

Table 2. Summary of Significant Findings with the Nanometal Oxide/Halogen Adducts Studied Herein[a]

adduct	halogen content wt % (TGA)	air stability	UV/vis absorption λ_{max} (nm)	Raman energy shift (cm^{-1})
NA-Al_2O_3/Cl_2 Plus	14	N/A	coincides with NA-Al_2O3 Plus	N/A
NA-Al_2O_3/Br_2 Plus	15	good	275, 390 (sh)	286
NA-Al_2O_3/I_2 Plus	18	very good	294, 373	192
NA-Al_2O_3/ICl Plus	35	good	229, 345 (sh), 475	200, 325
NA-Al_2O_3/IBr Plus	28	good	306, 500 (sh)	194, 218
NA-Al_2O_3/ICl_3 Plus	37	good	238, 345	334, 280
NA-TiO_2/Cl_2	3	N/A	coincides with NA-TiO_2	N/A
NA-TiO_2/Br_2	5	very poor	340	307
NA-TiO_2/I_2	13	poor	500 (b)	196
NA-TiO_2/ICl	19	very poor	330, 470	196, 340
NA-TiO_2/IBr	15	very poor	317, 490 (sh)	199, 241
NA-TiO_2/ICl_3	12	very poor	313	342
NA-CeO_2/Cl_2	2	N/A	coincides with NA-CeO_2	N/A
NA-CeO_2/Br_2	3	good	350 (b)	279
NA-CeO_2/I_2	5	very good	405 (b)	177
NA-CeO_2/ICl	4	good	350, 520	196, 320
NA-CeO_2/IBr	4	good	350, 475 (sh)	196, 233
NA-CeO_2/ICl_3	4	good	350, 525 (sh)	343
AP-MgO/Cl_2	7	good	coincides with AP-MgO	492
AP-MgO/Br_2	16	very good	280, 340	251
AP-MgO/I_2	21	very good	450 (b)	170
AP-MgO/ICl	22	very good	480 (b)	183
AP-MgO/IBr	44	very good	250, 450	195, 222
AP-MgO/ICl_3	37	very good	270	322

[a] N/A = not applicable. sh = shoulder. b = broad.

to the adsorbed interhalogen (ICl, IBr, and ICl_3), while the set of two peaks at lower binding energy coincides with that of the free adsorbed iodine, I_2 (Figure 4(2), (4), (5), and (6)). In the case of NA-Al_2O_3/IBr Plus, a set of peaks corresponding to adsorbed Br_2 was also observed. Interhalogen molecules, such as ICl and IBr, are known to contain I_2 as well as Cl_2 or Br_2 (for ICl and IBr, respectively) in their vapor phase, supporting our findings.[73] These results are further supported by the literature,[17] where it has been reported that IBr adsorbed on MgO decomposes forming I_2 and Br_2. In addition, Nagasao and co-workers reported decomposition of ICl adsorbed on silica into I_2 and release of the lighter halogen, Cl_2.[23] This finding also helps explain why we did not observe any peak corresponding to Cl_2 in either the ICl or the ICl_3 adduct, because the light Cl_2 has apparently been released from the surface. The origin of the free halogen, I_2, is probably caused by a combination of the following processes: (1) the presence of I_2 and Cl_2 (or Br_2) in the vapor phase of the interhalogens that would have been directly adsorbed onto the surface, (2) it was formed due to partial spontaneous decomposition upon adsorption, or (3) it was formed under the influence of the X-ray radiation, leading to a larger fraction of free I_2 on the surface. Because XPS is a technique that analyzes only the top several nanometers of the sample and can change the sample due to the measurement, these data are not to be considered representative for the quantitative content of the halogens and their state in the samples. Thus, the interhalogen versus halogen content was not analyzed and reported.

Table 2 summarizes the important findings of the studied materials. The obtained data of aerogel prepared (AP)-MgO adducts from Stoimenov et al.[8] have also been included for a more complete comparison.

B. Applications of Prepared Adducts. When compared to the previously studied adducts from nanosized MgO, the adducts studied in this Article tend to release elemental halogen more readily, especially the TiO_2 adducts. During the design of future applications, this difference in stability would need to be considered to obtain the best performance possible for the application. Their use as halogen transfer agents in organic/inorganic synthesis certainly is a possible use, as well as their use as powerful solid-state biocides.

Conclusions

We herein have described the straightforward synthesis of halogen (Cl_2, Br_2, and I_2) and interhalogen (ICl, IBr, and ICl_3) adducts of three different nanosized metal oxides (NA-Al_2O_3 Plus, NA-TiO_2, and NA-CeO_2), as well as their characterization utilizing several different techniques, including UV−vis, Raman, and X-ray photoelectron spectroscopies and thermogravimetric analysis. The synthetic procedure can be scaled up and large quantities produced for future applications, such as a safe way to store intact halogen/interhalogen, for use as halogenating agents in organic/inorganic synthetic reactions, or in the use as agents against vegetative cells, spores, and viruses.

We conclude that different nanosized metal oxides interact with various adsorbing strengths with the halogen/interhalogens used in our experiments, and this can be used to an advantage in the design of an adduct with specific characteristics, such as with a very strong interaction between the ionic metal oxide surface and the halogen/interhalogen, which could be used as a safe way to store intact halogen/interhalogen for longer periods of time. As a contrast, it may be useful to have a weaker interaction between the metal oxide and the halogen/interhalogen to give a potent biocide with a strong oxidizing power of the released halogen/interhalogen. There are many possibilities to fine-tune the adducts and thus for the use of such prepared compounds in various applications.

The prepared adducts show significant differences in their electronic transitions, which along with their altered vibrational frequency values indicate changes in the chemical

properties of the prepared adducts, giving rise to new possible applications.

The interaction between the ionic metal oxide surface and the halogen/interhalogen is concluded to be that of a strained halogen/interhalogen bond and with no formation of new surface species, such as halogen salts. This leads to a weakened halogen/interhalogen bond, causing a lowering of the Raman band for the halogen/interhalogen moiety, which is easily detected. In addition, Raman spectroscopy and XPS also confirm that, in some cases, the interhalogen adducts contain I_2 in addition to the interhalogen molecule on the surface.

No evidence of lowering of the Cl_2 stretch is observed for any of the three metal oxide chlorinated adducts investigated. The Cl_2 stretch is not detected at all in the Raman spectrum, but rather the evidence of formation of such chlorinated adducts lies in TGA, smell, increased biocidal activity, and EDX analysis (not shown), all indicating that chlorine is present in the three adducts, although no Raman peak is observed.

Overall, when NA-Al_2O_3 Plus, NA-TiO_2, and NA-CeO_2 are compared, the stability of the prepared halogen/interhalogen adducts varies significantly. When exposed to air, the adducts of NA-TiO_2 are the least stable, whereas the stability of the adducts based on NA-Al_2O_3 Plus and NA-CeO_2 is similar.

Also, in general, the strength of interaction with the oxides lies in the order of $I_2 > ICl > IBr \approx Br_2 > ICl_3$. The strength of interaction in the chlorinated adducts is difficult to quantify as these adducts have no significant color change from the starting materials and no halogen peak present in the Raman spectrum. Some of these data are summarized in Table 2.

We have observed a significant difference between nanosized and micrometer-sized metal oxides in this study. A comparison showed that the micronsized counterparts did not in any of the cases studied herein adsorb and retain any halogen, as compared to the nanosized materials that retained large amounts of halogen on the surface. We conclude that nanosurfaces are indeed different. They are chemically more active because of the significantly larger numbers of defects, edges, and apexes. Bulk materials consist of lower activity flat faces in the micrometer-size, leading to lower reactivities. In addition, nanomaterials have much larger surface areas, further increasing their reactivity.

Acknowledgment. Financial support from the Army Research Office through a DTRA grant and from the KSU Targeted Excellence Program is acknowledged with gratitude. We would also like to acknowledge the reviewers for their helpful comments and suggestions.

CM8000927